

Supporting Information

**Efficient and selective removal of Congo red by a C@Mo
composite nanomaterial using a citrate-based coordination
polymer as the precursor**

Xiao-Sa Zhang,^a Hong-Tian Zhao,^a Yu Liu,^a Wen-Ze Li,^{a*} Yan Wang,^a Xiao-Yu Zhao,^a
Ai-Ai Yang^a and Jian Luan^{b*}

^a College of Sciences, Shenyang University of Chemical Technology, Shenyang, 110142, P. R. China

^b College of Sciences, Northeastern University, Shenyang, 100819, P. R. China

E-mail: liwenze@syuct.edu.cn (W. Z. Li); 2010044@stu.neu.edu.cn (J. Luan)

Table S1 Selected bond distances (Å) and angles (°) for complex 1

Cu(1)–O(1)	1.934(5)	Cu(2)–O(1W)	2.089(5)
Cu(1)–O(5)	1.936(4)	Cu(2)–O(7)	1.912(4)
Cu(1)–O(4)	1.944(4)	Cu(2)–O(2)	1.921(5)
Cu(1)–O(7)	1.951(4)	Cu(2)–O(3)#2	1.923(5)
Cu(1)–O(6)#1	2.285(4)	Cu(2)–O(2W)	2.275(5)
O(1)–Cu(1)–O(5)	158.7(2)	O(7)–Cu(2)–O(2)	93.3(2)
O(1)–Cu(1)–O(4)	88.63(19)	O(7)–Cu(2)–O(3)#2	97.09(18)
O(5)–Cu(1)–O(4)	90.53(18)	O(2)–Cu(2)–O(3)#2	169.6(2)
O(1)–Cu(1)–O(7)	97.55(18)	O(7)–Cu(2)–O(1W)	135.79(19)
O(5)–Cu(1)–O(7)	84.59(17)	O(2)–Cu(2)–O(1W)	82.9(2)
O(4)–Cu(1)–O(7)	173.37(17)	O(3)#2–Cu(2)–O(1W)	88.7(2)
O(1)–Cu(1)–O(6)#1	94.6(2)	O(7)–Cu(2)–O(2W)	136.04(18)
O(5)–Cu(1)–O(6)#1	106.6(2)	O(2)–Cu(2)–O(2W)	86.7(2)
O(4)–Cu(1)–O(6)#1	87.89(17)	O(3)#2–Cu(2)–O(2W)	86.8(2)
O(7)–Cu(1)–O(6)#1	89.20(17)	O(1W)–Cu(2)–O(2W)	87.89(18)

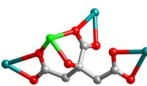
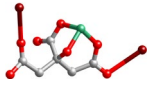
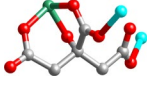
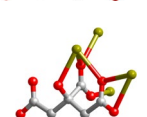
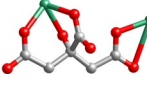
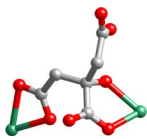
Symmetry code: #1 $-x + 2, y - 1/2, -z + 1/2$; #2 $x, -y + 3/2, z - 1/2$

Supporting Information

Table S2. Coordination Modes of Carboxylic Ligand H₄cit (Other Metal-based CPs)

No.	CP	cit anion	Coordination mode	Coordination mode of -COO group	-OH	Reference
A4	[Gd(cit)(H ₂ O)]		Pentadentate	$\mu_2\text{-}\eta^1:\eta^1$ $\mu_2\text{-}\eta^1:\eta^1$ $\mu_2\text{-}\eta^1:\eta^1$ $\mu_1\text{-}\eta^1:\eta^0$	μ_1	S1
A5	[5Ba(Hcit) ₂ (H ₂ cit) ₂ ·6H ₂ O]·2H ₂ O		Biadentate	$\mu_1\text{-}\eta^1:\eta^0$	NA	
			Tetradentate	$\mu_0\text{-}\eta^0:\eta^0$ $\mu_2\text{-}\eta^2:\eta^1$ $\mu_3\text{-}\eta^2:\eta^1$ $\mu_1\text{-}\eta^1:\eta^0$ $\mu_2\text{-}\eta^2:\eta^1$		S2
A6	[5.5Pb(Hcit) ₃ (H ₂ cit) ₂ ·5H ₂ O]·4.5H ₂ O		Tetradentate	$\mu_1\text{-}\eta^1:\eta^0$ $\mu_2\text{-}\eta^2:\eta^0$ $\mu_2\text{-}\eta^1:\eta^0$	μ_1	
			Pentadentate	$\mu_2\text{-}\eta^1:\eta^1$ $\mu_3\text{-}\eta^3:\eta^1$ $\mu_3\text{-}\eta^2:\eta^1$	μ_1	S2
A7	[Na(OH ₂) ₆]·{[Na ₃ (OH ₂) ₈] ₃ [NaPd ₃ (cit) ₃] ₂ }·(H ₂ O)	 A separate diagram shows the coordination mode of the citrate anion to the Na ⁺ cation.	Sexadentate	$\mu_3\text{-}\eta^2:\eta^1$ $\mu_1\text{-}\eta^1:\eta^0$ $\mu_3\text{-}\eta^2:\eta^1$	μ_3	S3
A8	[FeCd ₂ (Hcit) ₂ (H ₂ O) ₂]		Tetradentate	$\mu_3\text{-}\eta^2:\eta^1$ $\mu_1\text{-}\eta^1:\eta^1$ $\mu_3\text{-}\eta^2:\eta^1$	μ_1	S4
A9	[Cd ₃ (Hcit) ₂ (H ₂ O) ₂]		Tetradentate	$\mu_3\text{-}\eta^2:\eta^1$ $\mu_1\text{-}\eta^1:\eta^1$ $\mu_3\text{-}\eta^2:\eta^1$	μ_1	S4
A10	[NiZn ₂ (Hcit) ₂ (H ₂ O) ₂]		Tetradentate	$\mu_3\text{-}\eta^2:\eta^1$ $\mu_1\text{-}\eta^1:\eta^1$ $\mu_3\text{-}\eta^2:\eta^1$	μ_1	S5
A11	[CoCd ₂ (Hcit) ₂ (H ₂ O) ₂]		Tetradentate	$\mu_3\text{-}\eta^2:\eta^1$ $\mu_1\text{-}\eta^1:\eta^1$ $\mu_3\text{-}\eta^2:\eta^1$	μ_1	S5
A12	[CoZn ₂ (Hcit) ₂ (H ₂ O) ₂]		Tetradentate	$\mu_3\text{-}\eta^2:\eta^1$ $\mu_1\text{-}\eta^1:\eta^1$ $\mu_3\text{-}\eta^2:\eta^1$	μ_1	S5
A13	[Ln(Hcit)(H ₂ O) ₂ ·2H ₂ O] (Ln = Sm, Gd, Er, Nd)		Tridentate	$\mu_3\text{-}\eta^2:\eta^1$ $\mu_2\text{-}\eta^1:\eta^1$ $\mu_1\text{-}\eta^1:\eta^0$	μ_1	S6

Supporting Information

A14	[NiCd(cit)(H ₂ O)]		Tetradentate	$\mu_3\text{-}\eta^2:\eta^1$ $\mu_3\text{-}\eta^2:\eta^1$ $\mu_1\text{-}\eta^1:\eta^1$ $\mu_1\text{-}\eta^1:\eta^0$	μ_1	S7
A15	[Ge(Hcit) ₂ Ba(H ₂ O) ₃]·3H ₂ O		Tridentate	$\mu_1\text{-}\eta^1:\eta^0$ $\mu_2\text{-}\eta^1:\eta^1$ $\mu_1\text{-}\eta^1:\eta^0$	μ_1	S8
A16	[Cu ₂ Ge(cit) ₂ (INH) ₂]·4H ₂ O		Tridentate	$\mu_2\text{-}\eta^1:\eta^1$ $\mu_1\text{-}\eta^1:\eta^0$ $\mu_2\text{-}\eta^2:\eta^0$	μ_1	S9
			Biadentate	$\mu_1\text{-}\eta^1:\eta^0$ $\mu_0\text{-}\eta^0:\eta^0$	μ_1	
A17	[M(Hcit)(H ₂ cit)(H ₃ cit)(H ₂ O)]·H ₂ O (M = La, Ce)		Tetradentate	$\mu_3\text{-}\eta^2:\eta^1$ $\mu_0\text{-}\eta^0:\eta^0$ $\mu_3\text{-}\eta^2:\eta^1$	μ_1	S10
			Tetradentate	$\mu_3\text{-}\eta^2:\eta^1$ $\mu_0\text{-}\eta^0:\eta^0$	μ_1	
A18	[Zn(Hcit)(phen)(H ₂ O)][Zn ₂ (Hcit)(phen) ₂ (H ₂ O) ₃]·13.5H ₂ O phen = 1,10-phenanthroline		Biadentate	$\mu_1\text{-}\eta^1:\eta^1$ $\mu_1\text{-}\eta^1:\eta^0$ $\mu_1\text{-}\eta^1:\eta^0$	μ_1	S11
A19	[Zn ₃ (Hcit) ₂ (phen) ₄]·14H ₂ O		Biadentate	$\mu_1\text{-}\eta^1:\eta^1$ $\mu_1\text{-}\eta^0:\eta^0$ $\mu_0\text{-}\eta^0:\eta^0$	NA	S11
A20	[Co ₈ (cit) ₄ (bbi) ₆ (H ₂ O) ₁₀]·7H ₂ O bbi = 1,1'-(1,4-butanediyl)bis(imidazole)		Pentadentate	$\mu_2\text{-}\eta^2:\eta^0$ $\mu_2\text{-}\eta^2:\eta^0$ $\mu_1\text{-}\eta^1:\eta^0$	μ_3	S12

Supporting Information

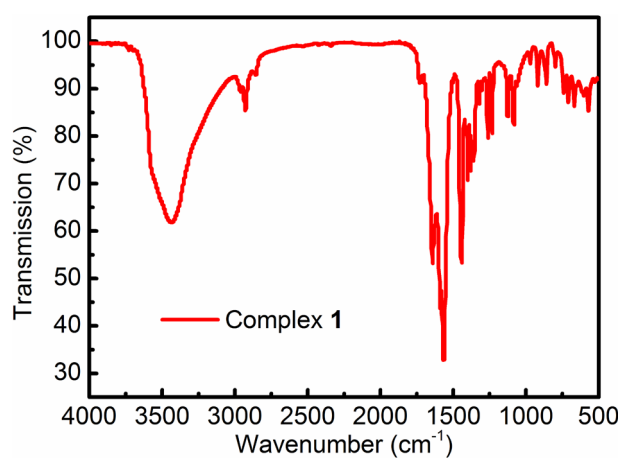


Fig. S1 The IR spectrum of complex **1**.

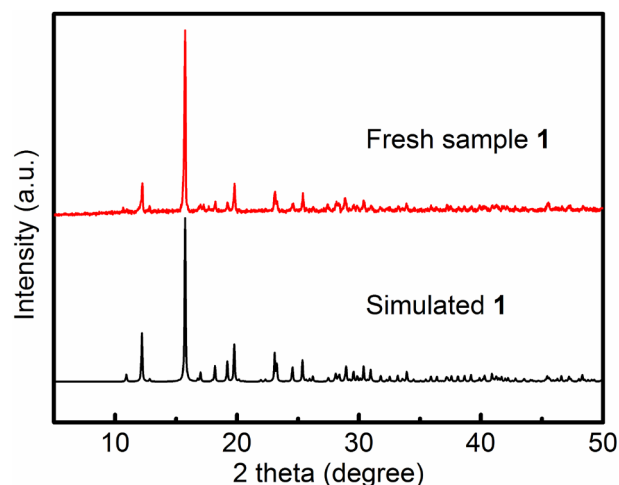


Fig. S2 The PXRD patterns of simulated and fresh sample for complex **1**.

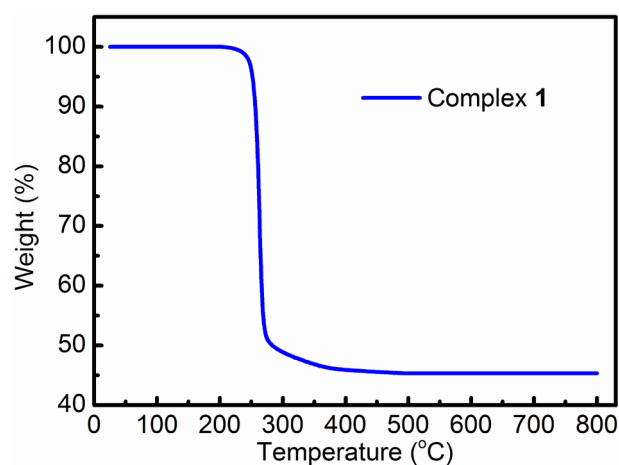


Fig. S3 The TG curve of complex **1**.

Supporting Information

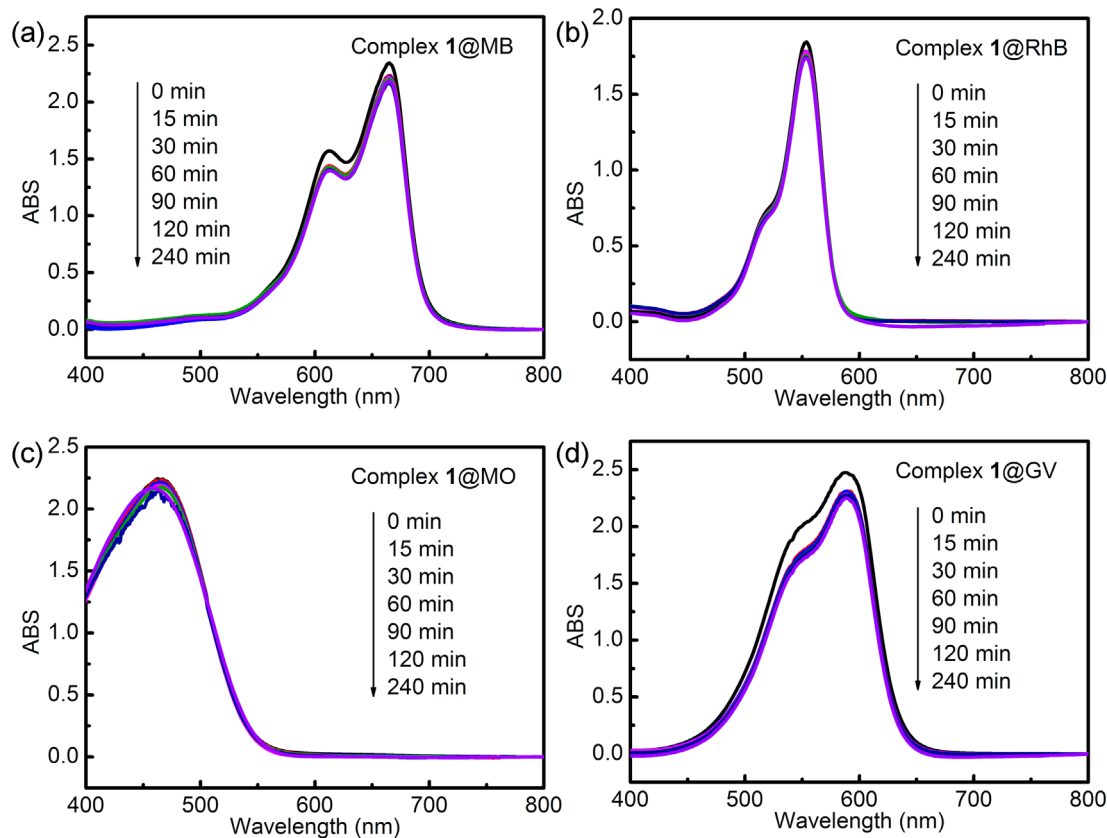


Fig. S4 UV–vis spectra of MB (a), RhB (b), MO (c), GV (d) solutions after different adsorption times with complex 1.

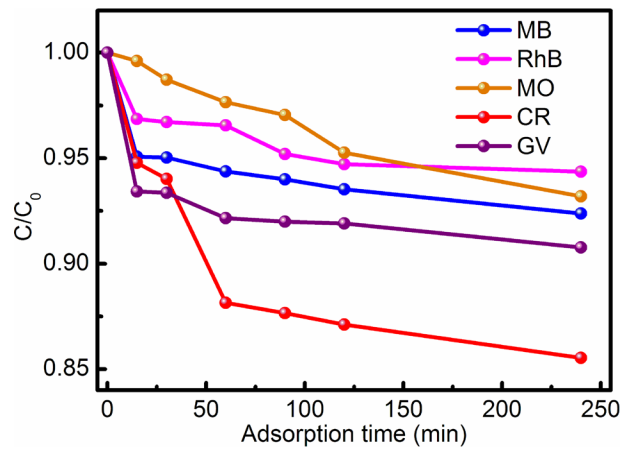


Fig. S5 The adsorption rates of MB, RhB, MO, CR and GV at different times with complex 1.

Supporting Information

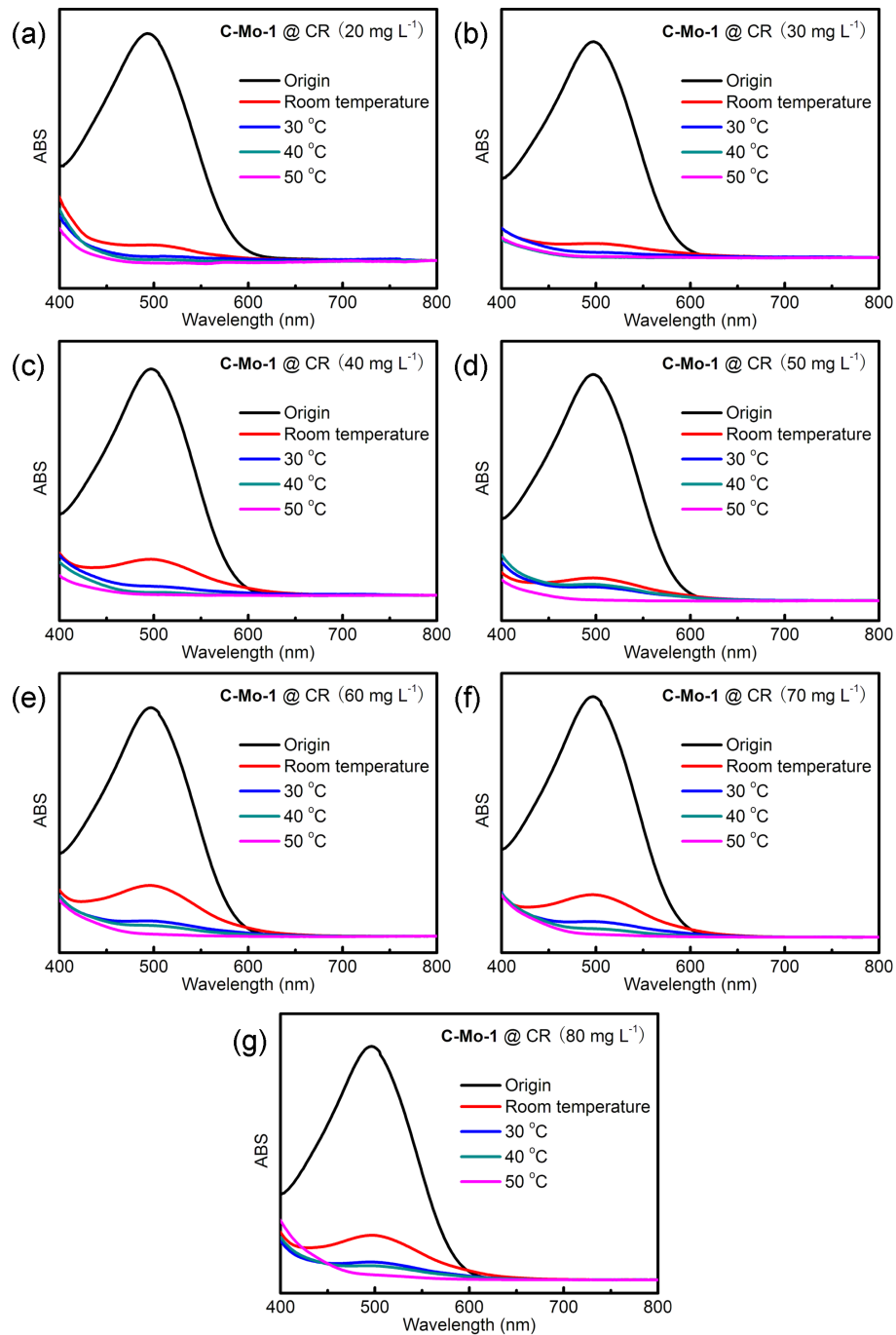


Fig. S6 UV-vis spectra of different concentrations of CR solutions after 240 min with **C-Mo-1** at different temperatures.

Supporting Information

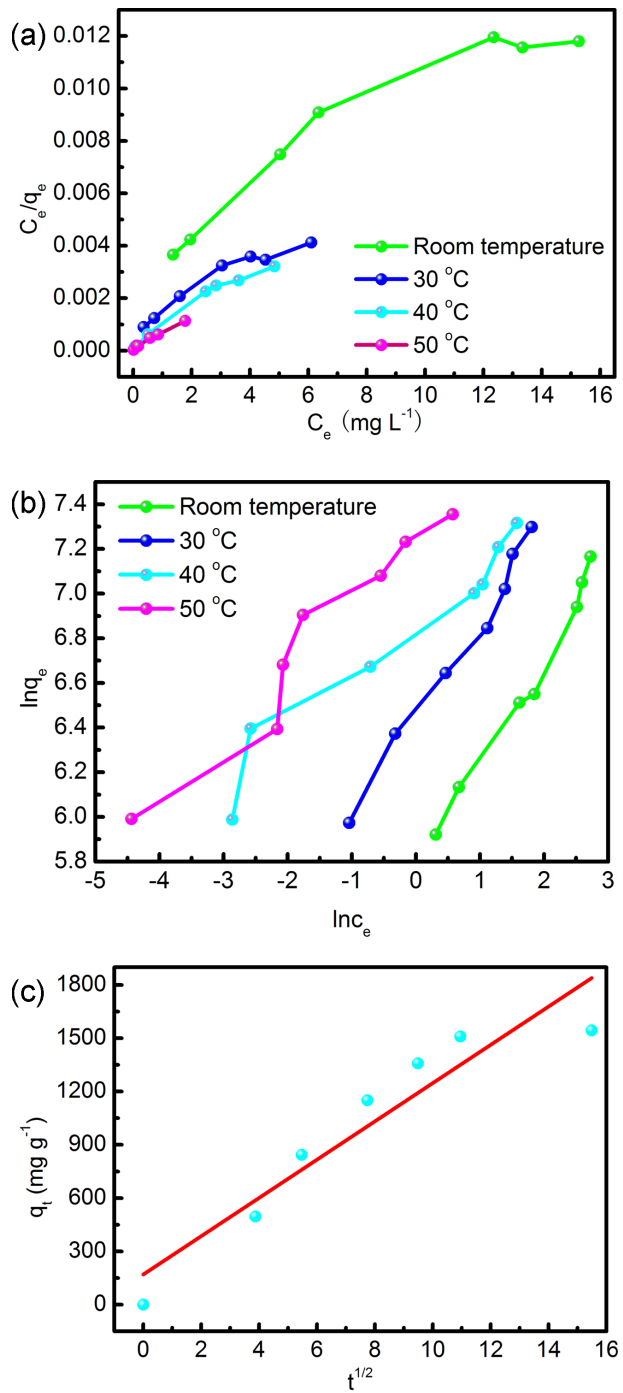


Fig. S7 Adsorption kinetics of CR adsorbed by **C-Mo-1**: (a) Pseudo-first-order model; (b) Pseudo-second-order model; (c) Intra-particle diffusion model.

Supporting Information

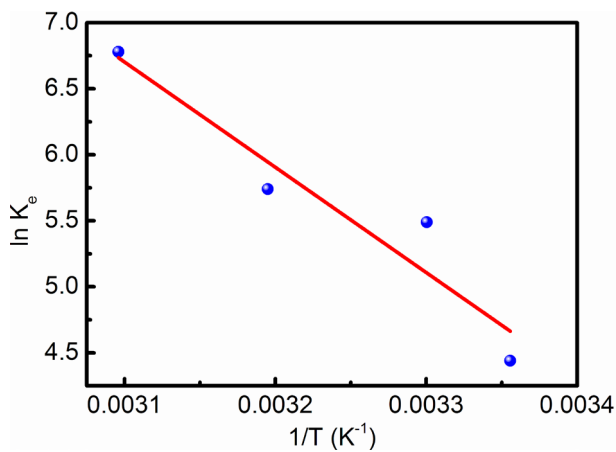


Fig. S8 The plot of $\ln K_e$ - $1/T$ for adsorption of CR on **C-Mo-1**.

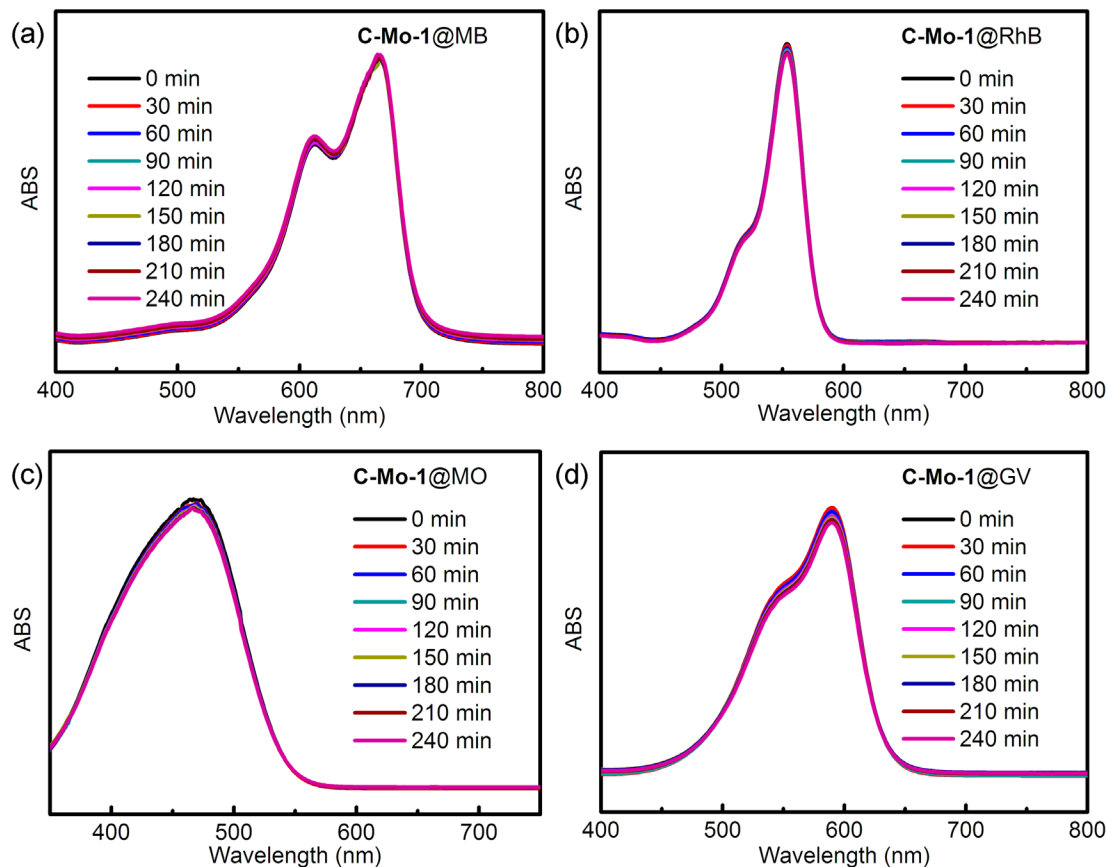


Fig. S9 UV-vis spectra of MB (a), RhB (b), MO (c) and GV (d) solutions after different adsorption times with **C-Mo-1**.

Supporting Information

Reference:

- S1 S. J. Liu, C. Cao, C. C. Xie, T. F. Zheng, X. L. Tong, J. S. Liao, J. L. Chen, H. R. Wen, Z. Chang and X. H. Bu, *Dalton Trans.*, 2016, **45**, 9209–9215.
- S2 A. Drzewiecka-Antonik, A. E. Koziol, P. Rejmak, K. Lawniczak-Jablonska, L. Nittler, T. Lis, *Polyhedron*, 2017, **132**, 1–11.
- S3 P. Gunari, S. Krishnasamy, S. Q. Bai and T. S. A. Hor, *Dalton Trans.*, 2010, **39**, 9462–9464.
- S4 L. Li, J. Jin, Z. F. Shi, L. M. Zhao, J. C. Liu, Y. H. Xing and S. Y. Niu, *Inorg. Chim. Acta*, 2010, **363**, 748–754.
- S5 L. Li, S. Y. Niu, J. Jin, Q. Meng, Y. X. Chi, Y. H. Xing and G. N. Zhang, *J. Solid State Chem.*, 2011, **184**, 1279–1285.
- S6 X. F. Li, Y. Y. Wu, H. J. Lun, H. Y. Li, J. H. Yang and Y. M. Li, *Synthetic Met.*, 2017, **232**, 103–110.
- S7 O. Mtoui-Sghaier, R. Mendoza-Meroño, E. Fernández-Zapico, S. García-Granda, A. Fernández-González, L. Ktari and M. Dammak, *J. Mol. Struct.*, 2016, **1105**, 105–111.
- S8 A. G. Pesaroglo, E. E. Martsinko, L. K. Minacheva, I. I. Seifullina and V. S. Sergienko, *Rus. J. Inorg. Chem.*, 2010, **55**, 1366–1372.
- S9 I. I. Seifullina, E. E. Martsinko, E. A. Chebanenko, V. V. D'yakonenko, S. V. Shishkina and O. V. Pirozhok, *J. Struct. Chem.*, 2018, **59**, 154–159.
- S10 S. F. Weng, Y. H. Wang and C. S. Lee, *J. Solid State Chem.*, 2012, **188**, 77–83.
- S11 R. H. Zhang, W. S. Xia, H. X. Wang and Z. H. Zhou, *Inorg. Chem. Commun.*, 2009, **12**, 583–587.
- S12 B. J. Zhang, C. J. Wang, G. M. Qiu, S. Huang, X. L. Zhou, J. Weng and Y. Y. Wang, *Inorg. Chim. Acta*, 2013, **397**, 48–59.